Geotechnical Aspects of Underground Construction in Soft Ground – Ng, Huang & Liu (eds)
© 2009 Taylor & Francis Group, London, ISBN 978-0-415-48475-6

Simulation of articulated shield behavior at sharp curve by kinematic shield model

J. Chen, A. Matsumoto & M. Sugimoto
Nagaoka University of Technology, Nagaoka, Niigata, Japan

ABSTRACT: Tunnelling cases at sharp curve have increased by using articulated shield with copy cutter. At sharp curve, the shield behavior, i.e., the position, the rotation angle, and the advance direction, should be precisely controlled to follow the planed alignment. However, it is sometimes difficult to control and predict the shield behavior without case records. To simulate the shield behavior, the kinematic shield model has been proposed by the authors, taking into account the excavated area, the tail clearance, the rotation direction of cutter face, the shield slide, and the dynamic equilibrium condition. This paper reports the simulation results of the articulated shield behavior during excavation at a sharp curve. This study yields the following findings: 1) The kinematic shield model simulates the measured path of the shield reasonably; 2) The articulated angle, the copy cutter area and length are the predominant factors affecting the shield behavior.

1 INTRODUCTION

Recently, aiming at the completeness of city functions in urban areas, many infrastructures such as roadways, water supply systems, sewerage and electric power lines, etc. have been constructed densely. Due to spatial limitation, sometimes it is difficult to choose simply an ideal route for a new tunnel. On the other hand, with new techniques adopted continuously, shield tunneling method has achieved greatly. Under these circumstances, many shield tunneling cases at sharp curve have been reported. In the case of excavation at a sharp curve, articulated shield becomes popular since conventional single shield met some difficulties in operational control and generated wide range of ground disturbance.

The direction control systems have been applied. However, these systems are based on empirical relationships and are lacking in the precise theoretical background (Shimizu & Suzuki 1994). Therefore it is sometimes difficult to control the shield at a sharp curve and to predict the shield behavior without case records.

To clarify the shield tunneling behavior and the behavior of the surrounding ground, numerical methods such as FEM, DEM have been adopted (Komiya et al. 1999; Kasper & Meschke 2004; Melis & Medina 2005). The enforced displacement by means of the gap between the excavated surface and the tunnel lining has been applied in FEM and this technique gave a very good prediction of the ground movement for shield tunneling (Rowe & Lee 1992). DEM is proved to be effective for soil stability problem at tunnel face. However, these numerical methods require the shield movement as one of known conditions. The immediate ground movement during excavation stage is difficult to be simulated, since it is related to the shield movement and the excavated area.

By taking into account ground displacement around the shield, the kinematic shield model had been proposed for single circular shield (Sugimoto & Sramoon 2002). This model was validated by the simulation of an earth pressure balanced (EPB) shield behavior along a straight alignment in a single layer of sandy gravel (Sramoon et al. 2002) and along a curve in a multilayered ground (Sugimoto et al. 2007). Extending this model to articulated shield, the articulated shield model was developed and validated by simulating the steady behavior of curve-only excavation (Sugimoto et al. 2002).

The transient behavior of an articulated shield in a way of sharp curvature movement is of interest to be cleared. In this study, the simulation results of the articulated shield behavior at a sharp curve with radius 20 m are reported. The validity of the model is examined by comparing the simulation results with the measurement data. Furthermore, the factors affecting shield behavior are also discussed.

2 KINEMATIC SHIELD MODEL

The articulated shield model is composed of five forces: force due to self-weight of machine, f_1; force

on the shield tail, f_2; force due to jack thrust, f_3; force on the cutter disc, f_4; and force on the shield periphery, f_5, as illustrated in Fig. 1 (Sugimoto & Sramoon 2002). Among them, f_1 and f_5 act on both sections of the shield. f_3 comes from shield jacks and articulated jacks. f_5 is composed of the ground reaction force and the dynamic frictional force on the shield skin, which are due to the earth pressure acting on the shield skin plate. Since earth pressure is reliant on ground deformation, and excavated cross section area is usually a little bit larger than the shield cross section area, the ground reaction force from the ground to the shield can be obtained by considering the coefficient of earth pressure K, which is given by a function of the distance between the original excavated surface and the shield skin plate U_n, as shown in Fig. 2. In Fig. 2, K at $U_n = 0$ means the coefficient of earth pressure at rest K_0, and the gradient of K at $U_n = 0$ represents the coefficient of subgrade reaction k. Here, note that the subscripts h and v mean horizontal and vertical directions, respectively; the subscripts *min*, *o*, and *max* define minimum, initial, and maximum, respectively; and σ_{v0} is overburden pressure. K in any direction K_n can be calculated by interpolation between K_h and K_v.

The shield behavior is represented by the movement of the shield in x, y, and z directions (Δx, Δy, Δz), and the shield postures (yawing angle ϕ_y, pitching angle ϕ_p, and rolling angle ϕ_r). Since the change of ϕ_r is limited in practice, the factor of shear resistance due to the cutter torque α_{sg} was adopted as a parameter instead of ϕ_r.

The articulated shield behaviour can be obtained by solving the following equilibrium conditions of forces and moments:

$$\begin{bmatrix} \sum_{i=1}^{5} \left(\boldsymbol{F}_{Fi}^{M} + \boldsymbol{F}_{Ri}^{M} \right) \\ \sum_{i=1}^{5} \left(\boldsymbol{M}_{Fi}^{M} + \boldsymbol{M}_{Ri}^{M} \right) \end{bmatrix} = 0 \tag{1}$$

where $\boldsymbol{F}$ and $\boldsymbol{M}$ are the force and moment vectors and the subscripts F and R denote front and rear sections of the shield respectively. The moment vectors are generated by the cross product of the position

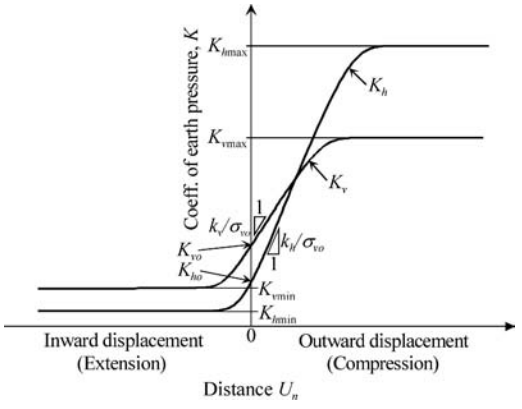

Figure 2. Ground reaction curve.

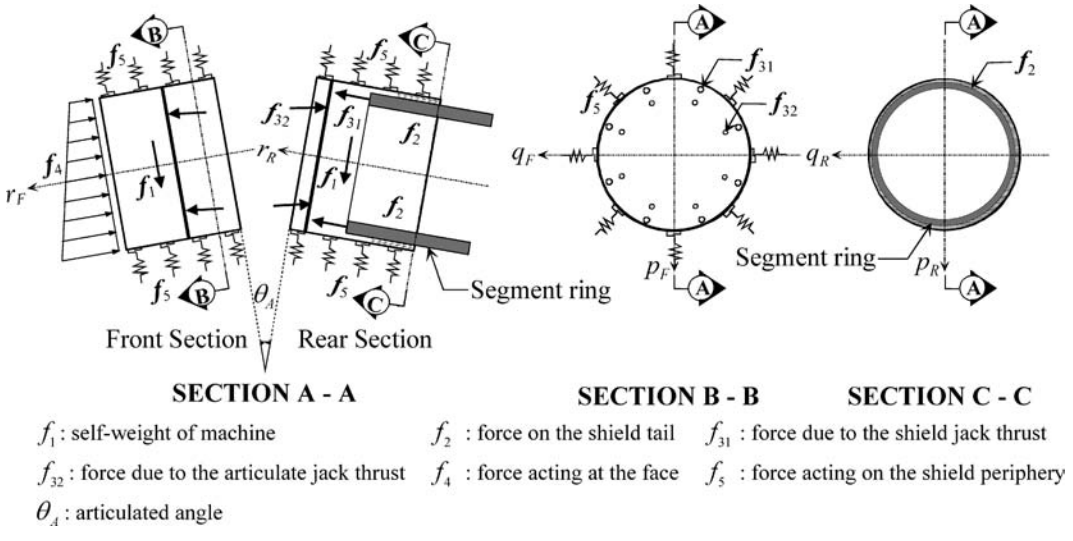

Figure 1. Model of loads acting on articulated shield.

vector and the force vector. Here, the superscript M indicates the machine coordinate system, which can be transformed to total coordinate system by using transformation matrices.

3 SHIELD TUNNELLING SITE

3.1 *Test site description*

The test site was established at a cable tunnel. The total length of this cable tunnel is 264 m and the test site is about 60 m long at a leftward sharp curve section with radius of 20 m. The inclined gradient of the tunnel alignment is upward of 0.2%.

Figure 3 shows the geological profile at the test section, where the overburden depth is about 34 m and the groundwater level is 2.8 m below the ground surface. Table 1 shows ground properties. The ground is composed mainly of alluvial layers (As1, Ac1, Acs, As2, and Ac2) and diluvial layers (Ds1, Dc2, Dc3, and Ds3). The tunnel is excavated in the diluvial sand layer Ds3 with N-values over 50 by standard penetration test.

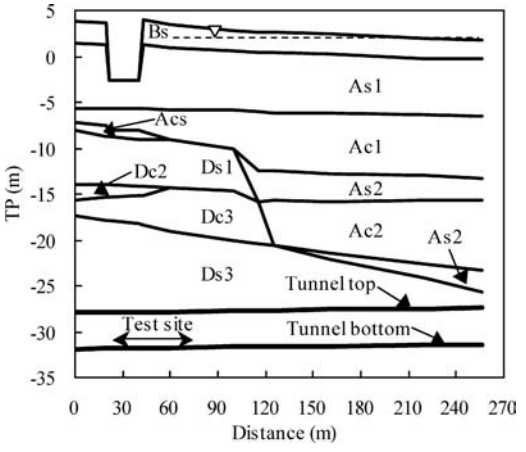

Figure 3. Geological profile at test site.

The articulated slurry shield with outer diameter of 3.95 m and 5.765 m in length was used. After excavation, the reinforced concrete segments with outside diameter of 3.8 m and 1.2 m in width were installed at the straight sections. The steel segments with 0.3 m in width were adopted at the curve section. The dimensions of the tunnel and the shield are summarized in Table 2.

Table 2. Dimension of tunnel and machine.

Item	Component	Value
Tunnel	Horizontal curve radius (leftward)	20 m
	Vertical slope gradient (ascending)	0.2%
	Overburden depth	34 m
	Groundwater level	G.L. −2.8 m
	Outer radius of segment	1.9 m
	Width of segments	1.2 m, 0.3 m
Shield	Outer radius	1.975 m
	Total length	5.765 m
	Length of front section	2.24 m
	Length of rear section	3.525 m
	Self-weight	810 kN
	Open ratio of cutter face	20.0%
	Thickness of cutter face	0.35 m
	Radius of chamber	1.943 m
	Length of chamber	0.80 m
	Radius of cutter face	1.98 m
Shield jack	Number of jacks	12
	Cross-sectional area	346.361 cm^2
	Radius of jack	1.67 m
Articulated jack	Number of jacks	12
	Cross-sectional area	433.736 cm^2
	Radius of jack	1.47 m

Table 1. Soil parameters at test site.

Soil layer	Unit weight γ(kN/m^3)	Cohesion c (kN/m^2)	Friction angle ϕ(°)	Coef. of subgrade reaction k (kN/m^3)	Coef. of earth pressure at rest K_0	Young's modulus E (kN/m^2)
Bs	19.0	0	26	4737	0.562	8400
As1	19.0	0	38	9474	0.384	16800
Ac1	15.3	59	0	789	0.844	1400
Acs	18.1	0	24	3158	0.593	5600
As2	19.2	0	29	7895	0.515	14000
Ac2	15.4	50	0	2368	0.832	4200
Ds1	19.2	0	37	19737	0.398	35000
Dc2	15.8	91	0	8684	0.848	15400
Dc3	15.0	160	0	7895	0.847	14000
Ds3	19.7	0	45	67895	0.293	120400

3.2 *In situ data*

Figure 4 shows the data of tunneling operation, shield behavior, and excavation condition measured continuously by automatic measurement system. The parameters of tunneling operation are articulated angle in horizontal direction θ_{CH} (+: leftward), area of applied copy cutter *CC* range (measured from the invert of shield in clockwise direction, viewed from shield tail), jack thrust F_{3r}, horizontal jack moment M_{3p} (+: rightward), vertical jack moment M_{3q} (+: downward), and cutter torque *CT* (+: anticlockwise direction, viewed from shield tail). The parameters of observed shield behavior are defined as yawing angle ϕ_y (+: rightward), pitching angle ϕ_p (+: downward), and rolling angle ϕ_r (+: clockwise direction, viewed from shield tail). The parameters of excavation condition are shield velocity v_s, slurry pressure σ_m, and slurry density γ_m in the chamber, which are usually controlled to stabilize the tunnel face. The mucking ratio R_v is the ratio of the measured discharged soil volume to the theoretical excavated soil volume.

The articulation of the shield was applied to negotiate the sharp curve. To follow the planed alignment, the applied articulated angle increased gradually from the beginning point of the curve, then it kept steady value of 500 minutes, which suits for the leftward curve of 20 m radius. *CC* was approximately 0.1 m in length and was applied mainly in range of 30°∼180° (measured from the shield invert in clockwise direction, viewed from tail) to increase the excavated area around the cutter disc, which reduces the acting earth pressure on the shield skin plate and makes a shield advance easily. F_{3r} was applied to drive the shield forward against the earth pressure at the cutter face and the dynamic friction around the shield skin plate. After the transient section from curve to straight line (from the distance 75 m to the distance 80 m), F_{3r} increased obviously. M_{3p} was applied to turn the shield to follow the horizontal leftward curve. M_{3q} was mainly applied against the vertical moment due to the earth pressure on the cutter disc and the self-weight of the shield. *CT* was generated due to the shearing resistance on the cutter disc.

The observed ϕ_y reveals the detailed yawing behavior of the shield. The observed ϕ_p indicates that the shield negotiates the inclination of the tunnel alignment. The observed ϕ_r fluctuates at the sharp curve alignment and is somewhat relative to *CT* and the rotation direction of the cutter disc. This points out that the shield rolls around its longitudinal axis in the opposite rotation direction of the cutter disc.

The shield velocity v_s decreased at the sharp curve. To stabilize the face, σ_m was applied based on the lateral earth pressure at the tunnel face, and γ_m was kept approximately 12 kN/m^3. R_v was close to unity throughout the test site, which indicates that excellent excavation control has been achieved.

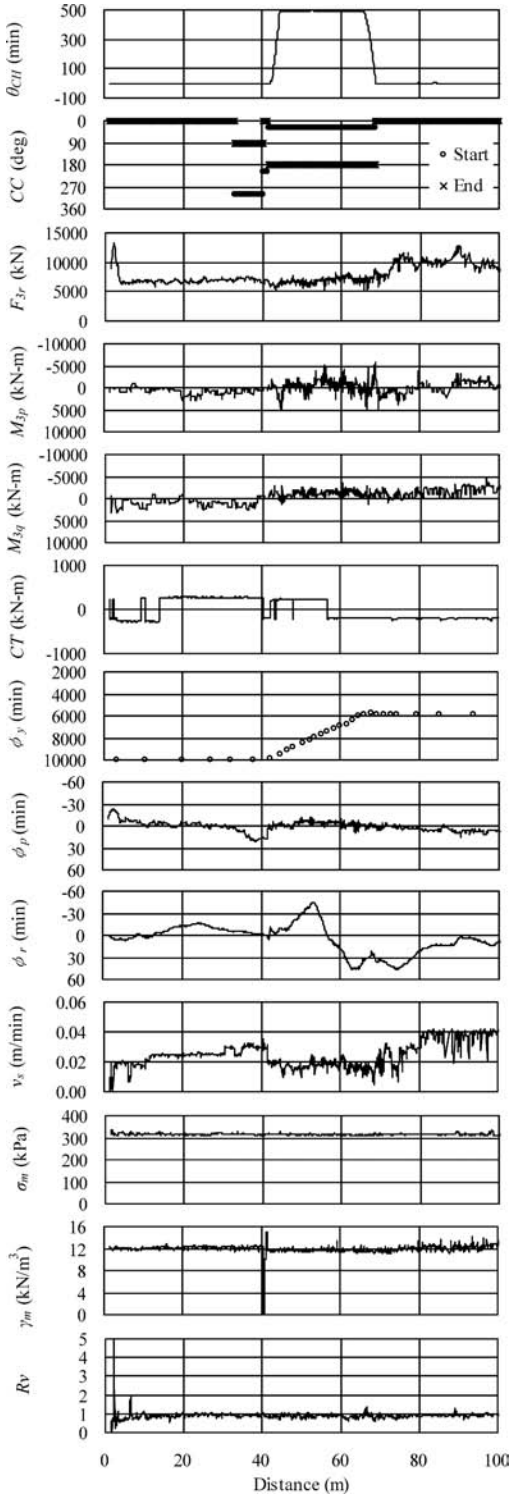

Figure 4. Shield tunneling measurement data.

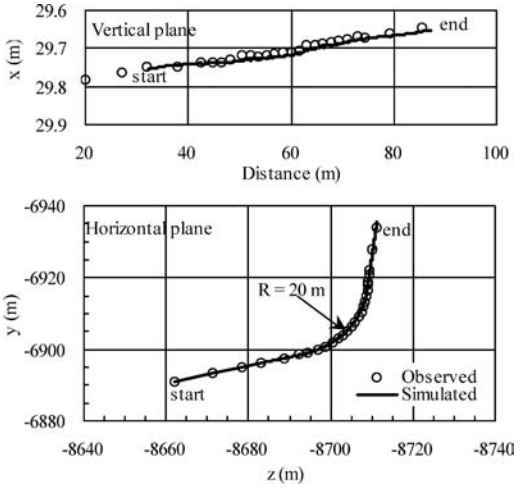

Figure 5. Simulated and observed shield traces.

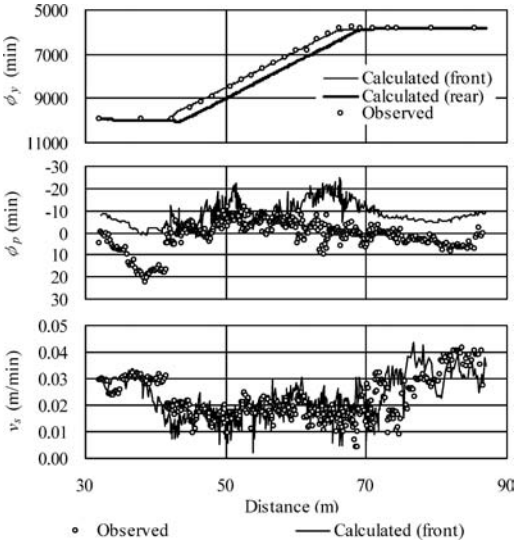

Figure 6. Simulated and observed shield behavior.

4 SIMULATION RESULTS

4.1 *Shield behavior*

Figure 5 shows the simulated and observed shield traces. From this figure, the maximum difference of 1 cm for vertical position and the maximum difference of 3 cm for horizontal position can be verified. The simulated and observed time dependent parameters ϕ_y, ϕ_p, v_s are compared in Fig. 6. The simulated ϕ_y indicates that the shield performs good negotiation to the sharp curve. As for the simulated ϕ_p, there is about 15 minutes uplift at the first straight section (from the distance 30 m to the distance 42 m), compared with the observed data. From the distance 60 m to the end point of the test site, maximum 20 minutes uplift can be found. Considering the possibility of change of geological conditions at some locations and the 5 minutes precision of the inclinometer, these differences are acceptable. Except for the transient section from curve to straight line, the calculated v_s is generally consistent with the observed. At the transient section, the maximum difference of 0.01 m/min for v_s is revealed. According to the construction report, intermittent excavation is applied to confirm the tail clearance at this section, there is some possibility to record slower velocity than that obtained in the simulation.

4.2 *Ground-shield interaction*

Ground-shield interaction is discussed by using the calculated distance between the original excavated surface and the shield skin plate U_n and the calculated normal effective earth pressure acting on the shield σ_{ns} at straight line and sharp curve. Figs. 7 and 8 show the distribution of U_n and σ_{ns} around the shield periphery at the straight line with distance of 39.3 m and at the sharp curve with distance of 58.4 m respectively. Here, note that the shield periphery is unfolded as a flat plate, i.e., the vertical axis shows the length of the shield and the horizontal axis represents the circumference of the shield.

In the case of excavation at straight line, the following are found from Fig. 7: (1) the contour lines of U_n become dense around 45°, 80°, 260°, 335° and U_n is about 30 mm around 60° and from 270° to 300°, because the copy cutter is applied from 300° to 90° shown in Fig. 4 and the effective rate of over cutting decreased between 30° and 330° by the assumption that the mucking at the invert is not sufficient; (2) the distribution of U_n at the cross section of the shield is almost same along the longitudinal direction, which is natural at straight line; (3) The contour lines of σ_{ns} appear around the invert and the crown of shield, since U_n around both spring lines is smaller than U_n at other area and the horizontal effective earth pressure is smaller than the vertical one due to K_0 of $D_{s3} = 0.293$ shown in Table 1.

When shield excavated at sharp curve, the following are found from Fig. 8: (1) U_n becomes positive at the end of the front body and the rear body around the right spring line of shield. At the same time, U_n becomes positive at the middle length of the both bodies along the left spring line. The shield skin plate at these locations pushes the ground, whereas U_n at the opposite side becomes negative, where the earth pressure is in extension state. These characteristics result from the equilibrium condition and correspond to the leftward curve of the tunnel alignment; (2) the contour

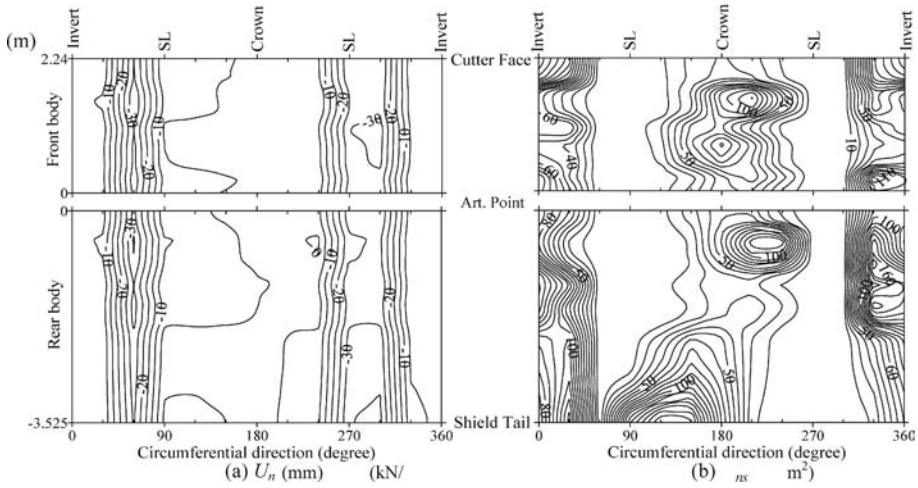

Figure 7. U_n and σ_{ns} around shield at the straight line with distance of 39.3 m.

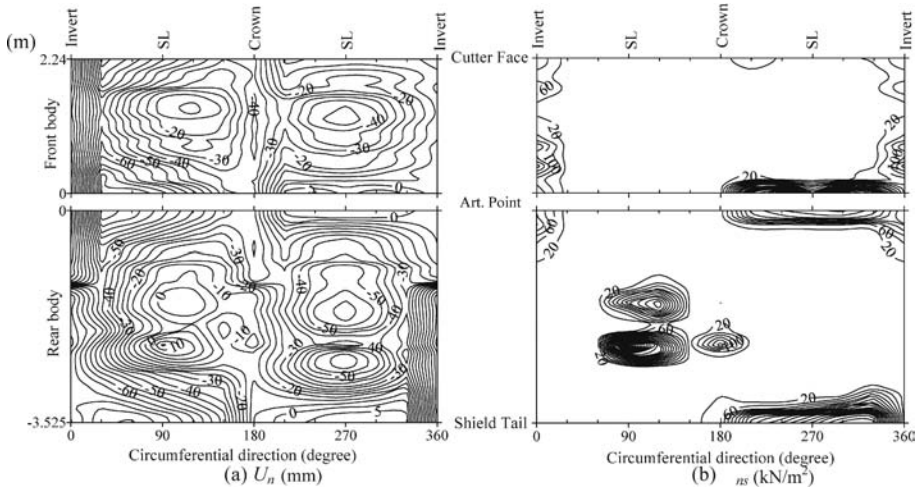

Figure 8. U_n and σ_{ns} around shield at the sharp curve with distance of 58.4 m.

lines of U_n become dense at the right bottom of the rear part and at the left bottom of the front part, since the applying range of copy cutter shifts at the boundary position due to the change of cutter face rotation direction shown in Fig. 4; (3) U_n along both spring lines has a fluctuation due to the wriggle motion of the shield during excavation; (4) the intensity of σ_{ns} appears at the area where U_n is positive, which is reasonable from the view point of ground-skin plate interaction.

5 CONCLUSIONS

The articulated shield behavior at sharp curve was simulated and the calculated shield behaviour was compared with the observed one. Furthermore, ground-shield interaction was discussed using the distribution of U_n and σ_{ns} around the shield. As a result, the following conclusions can be made:

1. The kinematic shield model for articulated shield simulated the shield position within 3 cm difference and the shield pitching angle within 20 minutes difference at sharp curve. This indicates that the proposed model can simulate shield behavior at sharp curve reasonably.
2. The articulated angle and the copy cutter area and length are the predominant factors affecting the shield behavior especially at sharp curve.

REFERENCES

Kasper, T. & Meschke, G. 2004. A 3D finite element simulation model for TBM tunneling in soft ground. *International Journal for Numerical and Analytical Methods in Geomechanics* 28(14): 1441–1460.

Komiya, K., Soga, K., Akagi, H., Hagiwara, T. & Bolton, M. D. 1999. Finite element modelling of excavation and advancement processes of a shield tunnelling machine. *Soils and Foundations* 39(3): 37–52.

Melis, M. J. & Medina, L. E. 2005. Discrete numerical model for analysis of earth pressure balance tunnel excavation. *Journal of Geotechnical and Geoenvironmental Engineering* 131(10): 1234–1242.

Rowe, R. K. & Lee, K. M. 1992. Subsidence owing to tunnelling: II. Evaluation of prediction technique. *Canadian Geotechnical Journal* 29: 941–954.

Shimizu, Y. & Suzuki, M. 1994. Movement characteristics and control method of shield tunnelling machine of articulate type. *Transactions of the Japan Society of Mechanical Engineers* (Series C) 60(571): 141–148. (in Japanese)

Sramoon, A., Sugimoto, M. & Kayukawa, K. 2002. Theoretical model of shield behavior during excavation II: Application. *Journal of Geotechnical and Geoenvironmental Engineering* 128(2): 156–165.

Sugimoto, M. & Sramoon, A. 2002. Theoretical model of shield behavior during excavation I: Theory. *Journal of Geotechnical and Geoenvironmental Engineering* 128(2): 138–155.

Sugimoto, M., Sramoon, A., Konishi, S. & Sato, Y. 2007. Simulation of shield tunnelling behavior along a curved alignment in a multilayered ground. *Journal of Geotechnical and Geoenvironmental Engineering* 133(6): 684–694.

Sugimoto, M., Sramoon, A., Shimizu, T., Dan, A. & Kobayashi, T. 2002. Simulation of articulated shield behavior by in-situ data based on kinematic shield model. *Journal of Tunnel Engineering* 12: 471–476. (in Japanese)